water

MDPI

Article

Optimal Selection and Operation of Pumps as Turbines for Maximizing Energy Recovery

Lucrezia Manservigi [1], Mauro Venturini [1,*], Enzo Losi [1] and Giulia Anna Maria Castorino [2]

[1] Dipartimento di Ingegneria, Università degli Studi di Ferrara, Via Saragat 1, 44122 Ferrara, Italy; lucrezia.manservigi@unife.it (L.M.); enzo.losi@unife.it (E.L.)
[2] Dipartimento di Studi Umanistici, Università degli Studi di Ferrara, Via Paradiso 12, 44121 Ferrara, Italy; giuliaannamaria.castorino@unife.it
* Correspondence: mauro.venturini@unife.it

Abstract: A pump as turbine (PAT) can be a cost-effective and versatile solution to recover energy in several fields of application. However, its optimal exploitation requires a reliable and general methodology for selecting the optimal turbomachine. To this purpose, this paper presents and validates a comprehensive methodology that identifies the best turbomachine (i.e., the one that maximizes the recovered energy) by considering two hydraulic sites and forty-five PATs. In both sites, the methodology correctly identifies the best PAT, which allows for the recovery of up to 45% of the available hydraulic energy. To further investigate PAT potential, an additional layout of installation, which comprises two PATs installed in parallel, is also considered. The operation of both PATs is optimally scheduled to maximize energy recovery. As a result, the energy recovered by the best pair of PATs is almost 50% of the available hydraulic energy. An in-depth analysis about PAT operation (i.e., operating range, causes of wasted energy, timeframe of operation and PAT efficiency) reveals that the installation of two PATs is actually recommended in just one of the two considered sites.

Keywords: energy recovery; pump as turbine; renewable energy; selection; operation

Citation: Manservigi, L.; Venturini, M.; Losi, E.; Castorino, G.A.M. Optimal Selection and Operation of Pumps as Turbines for Maximizing Energy Recovery. *Water* **2023**, *15*, 4123. https://doi.org/10.3390/w15234123

Academic Editor: Helena M. Ramos

Received: 30 October 2023
Revised: 20 November 2023
Accepted: 22 November 2023
Published: 28 November 2023

1. Introduction

In the last few years, the pump as turbine (PAT), i.e., a pump running in reverse mode, is gaining more and more attention in the literature, since it is a sustainable solution to recover energy in both industrialized and developing countries [1].

Thanks to their versatility, PATs are a suitable technology for several fields of application. In fact, they can be employed to replace conventional turbines in small-, micro- and pico-hydropower plants [2], since pumps are easier to maintain and retrieve [3]. In addition, a PAT is also significantly cheaper than a hydraulic turbine of comparable size, and the payback period is lower (estimated to be from 6 to 9 years, according to [4,5]).

In water transmission and distribution networks, PATs can be used to replace pressure reducing valves (PRVs) to reduce pressure by simultaneously reducing leakages and recovering exceeding energy that, instead, would be dissipated [6]. In fact, both recovered energy and leakage reduction may be noteworthy. For example, thanks to the installation of a PAT, the recovered energy was in the range from 32 MWh/year to 153 MW/year in studies [7–9], and annual leakages were decreased by 21% in [7].

PATs are also suitable for urban areas, e.g., neighborhoods [10], domestic water cycles [11] and low-temperature district heating networks [12], as well as for industrial sectors, e.g., irrigation and the mining and food industries [3]. For example, García et al. [13] investigated a hybrid system composed of one PAT and photovoltaic panels installed in a farm irrigation network, while Ji et al. [14] exploited a pump used in reverse mode in a demineralized water treatment system.

PATs are also a viable solution for storage purposes, as demonstrated in Wang et al. [15] in which a low-head pumped hydro energy storage exploits an axial-flow PAT.

Despite the aforementioned advantages, the actual effectiveness of exploiting PATs is usually limited by the fact that the selection of the optimal turbomachine is still a complex and challenging task [16,17]. The selection of an improper PAT leads to dramatic consequences, as proved by Venturini et al. [8] who analyzed different PAT–site matches. In fact, the best PAT recovered 40% of site hydraulic energy, while the energy recovery by means of the second-best and third-best PATs was equal to 19% and 3%, respectively. Finally, the energy production by means of the fourth PAT was null. This paper will quantitatively assess the effect of an improper PAT–site matching both for a single PAT and a pair of PATs. In fact, only the installation of the best PAT allows for the pursuit of two relevant targets set by the EU [18], i.e., sustainability and efficiency improvement.

The interest in this research field is proven by the following recent studies, which are aimed at developing methodologies for the selection of an optimal PAT as a function of the characteristics of a given hydraulic site.

Balacco et al. [16] developed a tool that guides the selection of the optimal PAT through three steps. First, site characteristics are defined, and the average of daily water demand is assumed to be the best efficiency point (BEP) of the PAT. Then, the required pump is identified based on its BEP, which is estimated by means of empirical equations. Finally, PAT characteristic curves should be employed to assess the actual energy recovery. The methodology proposed in Stefanizzi et al. [19] was aimed at selecting the optimal pump from commercial catalogues by means of the PAT's specific speed, which can be calculated by using site characteristics (i.e., mean flow rate and mean head). Novara and McNabola [20] discretized the hydraulic site domain in which each flow rate and head coordinate corresponds to the BEP of an ideal PAT. The characteristic curve of each ideal PAT is derived at a given rotational speed. For each ideal PAT, the expected yearly energy yield and payback time are calculated by using empirical equations available in the literature. The approach proposed by Pugliese and Giugni [21] provided the main features (i.e., BEP, impeller diameter and rotational speed) of the optimal PAT by assuming that it is operated with speed control. Marini et al. [17] developed a software that designs the optimal PAT suitable for three control strategies, i.e., hydraulic regulation, electric regulation and coupled hydraulic/electric regulation. Dimensionless energy is used to determine the optimal PAT in terms of recovered energy and costs. Nasir et al. [22] employed statistical models and Pearson correlation coefficients to grasp the relationship between site and optimal PAT. The methodology proposed in Barbarelli et al. [23] assumed that a PAT's BEP corresponds to the mean flow rate and head of the site. Kostner et al. [24] identified the ideal PAT by assuming that each flow rate of the water distribution network is the flow rate at BEP of the optimal turbomachine. Then, the pressure head is calculated by using empirical equations, and the PAT's BEP is transformed into the corresponding value in pump mode. Fernández García et al. [25] proposed novel indicators to estimate the recoverable energy by also assessing leakage reduction and water cost savings. Then, the payback period was estimated. In [26], Fernández García and Mc Nabola proposed an optimization methodology that provided the optimal number and location of PATs at each node of a water distribution network. A limitation of the methodology acknowledged by the authors is that the methodology is not suitable for complex looped networks because of the required computational time. Pérez-Sánchez et al. [27] performed PAT selection by means of the simulated annealing algorithm. Such a tool was also exploited in Garcia et al. [28]. Chacón et al. [29] developed an advanced statistical methodology to predict monthly flow fluctuations, which was used to estimate the PAT's working frequency at BEP. The PAT's optimal power was determined by minimizing the PAT's payback period. Finally, Pérez-Sánchez et al. [30] presented a novel strategy to optimize the recovered energy by using a best efficiency line, i.e., the line that connects the BEPs given the rotational speed and flow.

Despite the considerable number of studies dealing with the selection of the optimal PAT, none of them proved to be an indisputable benchmark to follow [19]. Indeed, in most cases, they are difficult to replicate at a different site. In addition, most methodologies

derive the PAT characteristic curves by means of an empirical correlation by introducing errors in the estimation of PAT performance [19] and energy recovery, accordingly.

This gap is filled by the current paper, which is aimed at (i) validating the selection methodology developed in Manservigi et al. [31] and (ii) assessing the potential of exploiting PATs for energy recovery. To these purposes, two installation layouts are investigated. The former comprises one PAT, while the latter accounts for two PATs installed in parallel. A bypass line is also included in both layouts. In the case that a pair of PATs is installed, the optimal operation of each turbomachine is scheduled to maximize recovered energy. The causes of wasted energy are also discussed. The PAT's operation is managed according to throttle or bypass control.

Finally, it has to be highlighted that this paper investigates the PAT's capability under an energy point of view, whereas economic evaluations are out of this paper's purposes.

The novelty of this paper can be summarized as follows:

- Validation of the methodology proposed in Manservigi et al. [31]. The validation is performed by means of two sites that differ in both flow rate and head characteristics by strengthening the general validity of the proposed methodology;
- Validation by means of the experimental characteristic curves of a fleet of forty-five PATs so that the recovered energy is calculated by exploiting the entire operating range of each turbomachine. Thus, this paper differs from state-of-the-art studies, which usually present the validation of the respective methodologies by means of predicted PAT characteristic curves;
- Operation of each pair of PATs is finely scheduled to maximize the recovered energy (15 min step time). Instead, some studies assume that each PAT continuously operates over a longer time slot (e.g., night or day).

It has to be highlighted that the results of this paper demonstrate the PAT's potential in terms of both sustainability and efficiency improvement. In fact, PATs are a sustainable solution to recover hydraulic energy that, in some cases, would be unexploited. Moreover, as demonstrated in the literature, PATs dissipate exceeding pressure by simultaneously reducing leakages. In addition, as quantitatively demonstrated in this paper in the Results Section, (i) identifying the best PAT, (ii) scheduling the optimal operation of each turbomachine and (iii) analyzing the causes of energy waste help to improve the PAT's efficiency.

This paper is structured as follows. First, the methodology for PAT selection and the rationale of the control strategy are described. Then, the case study is presented by defining the hydraulic sites, the considered PATs and the installation layouts. Then, the results are discussed by both validating the selection methodology and focusing on the operation of the best PATs (single PAT or pair of PATs). Finally, conclusions are drawn.

2. PAT Selection and Control

2.1. PAT Selection

In this paper, the best PAT (i.e., the one that maximizes the recovered energy) to install in a given site is selected by means of the methodology developed by Manservigi et al. [31], which is sketched in Figure 1.

The PAT selection methodology requires three inputs, i.e., (i) maximum flow rate (Q_{max}) and maximum head of the site (H_{max}); (ii) mean flow rate (Q_{mean}) and mean head of the site; and (iii) a fleet of pumps, among which the optimal PAT can be selected. For each pump of the fleet (i.e., N_P in total), the flow rate and head at BEP ($Q_{BEP,P}$, $H_{BEP,P}$) are known, since they can be derived from pump catalogues or experimental data.

First, for each PAT, the runaway condition, i.e., at the minimum flow rate, is calculated to filter out those PATs that are not suitable for the site under analysis. To this purpose, Manservigi et al. [31] derived Equations (1) and (2), which calculate the minimum flow rate of the PAT ($Q_{r,T}$) and the minimum head of the PAT ($H_{r,T}$) based on the BEP values of some PATs running in pump mode (i.e., $Q_{BEP,P}$ and $H_{BEP,P}$).

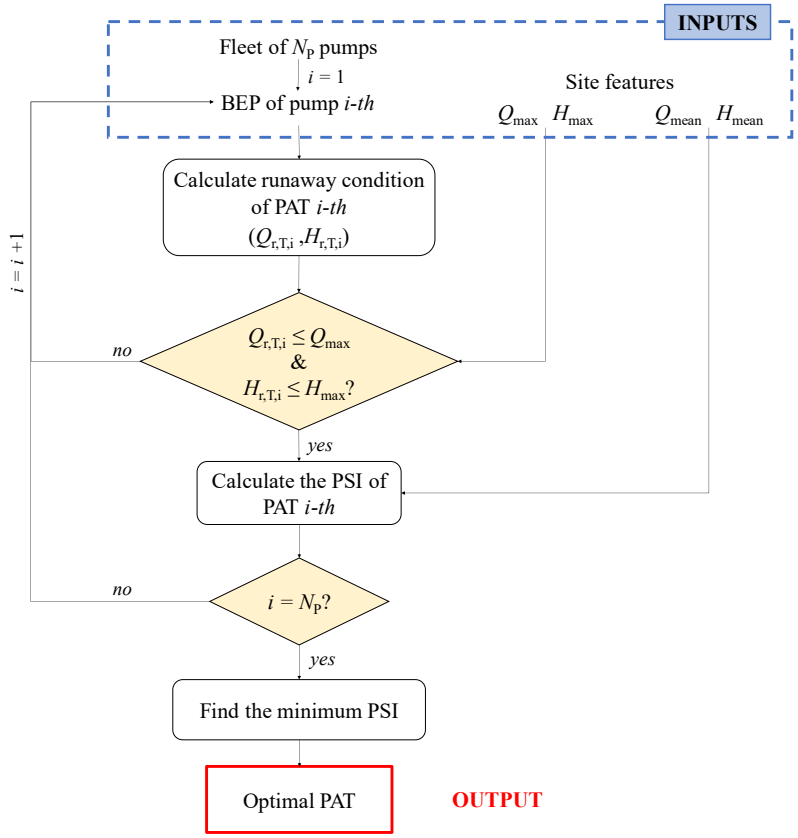

Figure 1. PAT selection methodology.

It has to be mentioned that (i) Equations (1) and (2) can be applied when the pump's BEP is in the range from 3 L/s to 130 L/s and from 1 m to 57 m; (ii) the PAT runaway condition and pump's BEP refer to the same rotational speed; and (iii) the flow rates in Equation (1) are expressed in L/s.

$$Q_{r,t} = 0.5856 \times Q_{BEP,P} + 2.0815 \quad (1)$$

$$H_{r,t} = 0.9710 \times H_{BEP,P} - 0.9877 \quad (2)$$

By assuming that a PAT operates at a constant rotational speed, the PATs of which the runaway condition exceeds the maximum flow rate or maximum head of the site are filtered out, since the recovered energy (E_{rec}) would be null.

Then, PAT selection is performed by calculating the PAT–site index (PSI), which is defined as in Equation (3) [31]:

$$PSI = \sqrt{(Q_{ratio} - Q_{ref})^2 + (H_{ratio} - H_{ref})^2} \quad (3)$$

where Q_{ratio} is the ratio of $Q_{BEP,P}$ to the mean flow rate of the site (Q_{mean}). Similarly, H_{ratio} is the ratio of $H_{BEP,P}$ to the mean head of the site (H_{mean}).

In Equation (3), Q_{ref} and H_{ref} are the reference flow rate and reference head, respectively. Q_{ref} is equal to 1.00, while H_{ref} is equal to 0.95. Such reference values were derived in Manservigi et al. [31] by using the sixteen PAT–site matches considered in [8]. In [8], the Q_{ref} of the best PAT–site matches was close to 1, while the H_{ref} of the best PAT–site matches was in the range from 0.5 to 1.4 with a mean value of 0.95.

The best PAT is the one that minimizes the PSI, since it is the closest to the reference condition.

2.2. PAT Control

For PAT control, throttle or bypass control [32], also known in the literature as "hydraulic regulation" [17] or "mechanical regulation" ([33]), can be employed. In this paper, the PAT's rotational speed is kept constant over time.

In water distribution networks, such a control entails that one PAT is installed in series with one PRV that regulates the head (Figure 2a). In addition, the presence of both a bypass line [34,35] and a three-way valve is also required.

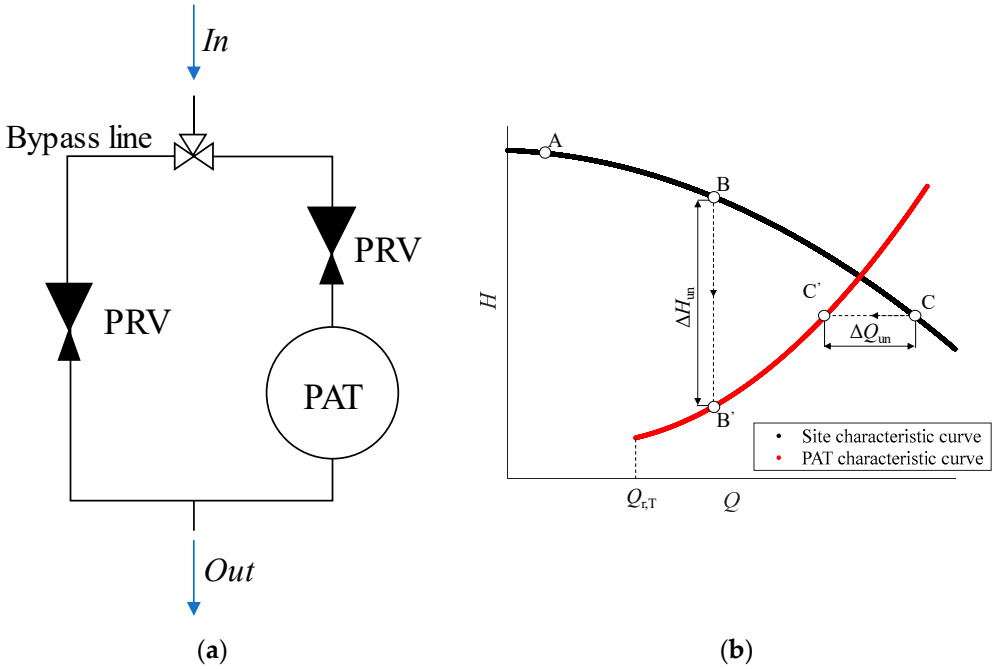

Figure 2. Layout of the installation of a single PAT and a bypass line (**a**); throttle and bypass control (**b**).

At each time step, both the flow rate and head must be adjusted by identifying three different scenarios (Figure 2b).

In the first scenario (e.g., point A in Figure 2b), the site flow rate is lower than the PAT's flow rate at runaway condition ($Q_{r,T}$). Thus, the entire flow rate passes through the bypass line, the PAT does not run, and consequently, the recovered energy is null.

The second scenario occurs when, for a given site flow rate, the PAT's head (H_{PAT}) is lower than the head of the site [32], e.g., point B in Figure 2b. In this case, a throttle control is used [32], and the exceeding head of the site is dissipated. The unexploited head (ΔH_{un}) is the difference between the head of the site and the PAT's head (Equation (4)), while the PAT swallows for the entire flow rate made available by the hydraulic site. Due to throttle control, part of the hydraulic energy is unexploited ($E_{un,TC}$) (Equation (4)).

$$\text{If } H_{PAT} \leq H_{site} \text{ then } \begin{cases} \Delta H_{un} = H_{site} - H_{PAT} \\ Q_{PAT} = Q_{site} \\ E_{un,TC} = (\rho \times g \times \Delta H_{un} \times Q_{site}) \times \Delta t \end{cases} \quad (4)$$

The third scenario occurs when, for a given site flow rate, the PAT's head H_{PAT} is higher than H_{site}, e.g., point C in Figure 2b. In such a case, a bypass control is performed: the PAT operates at the head of the site, and the exceeding flow rate is delivered through the bypass line. Thus, a part of the flow rate fraction is unexploited (ΔQ_{un}) by wasting the hydraulic energy $E_{un,BC}$ (see Equation (5)).

$$\text{if } H_{PAT} > H_{site} \text{ then } \begin{cases} \Delta Q_{un} = Q_{site} - Q_{PAT} \\ H_{PAT} = H_{site} \\ E_{un,BC} = (\rho \times g \times H_{site} \times \Delta Q_{un}) \times \Delta t \end{cases} \quad (5)$$

In throttle and bypass control, the recovered power (P_{rec}) is calculated by using the PAT's power characteristic curve, which can be derived experimentally (as performed in this paper) or by applying one of the methodologies available in the literature. To this purpose, different approaches can be exploited, e.g., physics-based approaches (e.g., [36,37]), empirical models (e.g., [23,38,39]), black box models (e.g., [40,41]), CFD models (e.g., [39,42]) and entropy production analysis (e.g., [43]).

Then, the recovered energy E_{rec} can be estimated according to Equation (6).

$$E_{rec} = \sum P_{rec} \Delta t \quad (6)$$

3. Case Study

In this paper, several PAT–site matches are analyzed by considering two sites and a fleet of forty-five PATs.

3.1. Sites

Two sites are simulated to mimic the experimental water distribution networks reported in [8]. The simulated sites, namely Site #1 and Site #2, are obtained by using the following procedure.

First, a second-order polynomial function interpolates experimental Q and H measurements to grasp the characteristic curve of the experimental site. Second, both Q and H noisy values are randomly generated within a range of which the bounds are equal to the standard deviation of the experimental site. Thus, each simulated Q value is obtained as the sum of an experimental and a noisy value. Then, the simulated Q feeds the characteristic curve of the experimental site, and an H noisy value is added. As a result, the simulated H is obtained.

As in [8], each simulated site covers one year of operation, and time granularity (i.e., Δt in Equations (4)–(6)) is equal to 15 min. Thus, each site accounts for 35,040 data points. All data are used to calculate the energy recovered by each PAT and, thus, validate the selection methodology.

The features of Site #1 and Site #2 are summarized in Table 1. Site #1 covers a broader range of Q, since the mean flow rate and maximum flow rate are approximately equal to 117 L/s and 303 L/s (Table 1), respectively. Instead, at Site #2, the flow rate is lower than 75 L/s. Conversely, Site #2 covers a higher range of head drop, since its maximum value is approximately equal to 66 m, i.e., roughly four-times higher than that of Site #1.

Table 1. Features of Site #1 and Site #2.

	Q_{mean} [L/s]	Q_{max} [L/s]	H_{mean} [m]	H_{max} [m]	E_{site} [MWh/Year]
Site #1	117	303	12	16	115
Site #2	28	75	46	66	101

As a result, the total hydraulic energy of the two sites (E_{site}) is roughly equal to 115 MWh/year (Site #1) and 101 MWh/year (Site #2); E_{site} is calculated as the sum of the hydraulic energy of each site data, i.e., $0.25 \cdot \rho \cdot g \cdot Q \cdot H$. The coefficient 0.25 accounts for time granularity that is equal to 15 min.

Site #1 and Site #2 exhibit a similar behavior over time (Figure 3). In fact, in both cases, the flow rate is minimum in the first hours of the day (i.e., slot 00:00–04:00), tends to increase especially from 04:00 to 08:00 and, finally, significantly decreases in the last hours of the day (i.e., slot 20:00–24:00). Conversely, head drop exhibits a decreasing trend from 08:00 to 16:00. Such overall behavior correctly reflects typical water demand values [32].

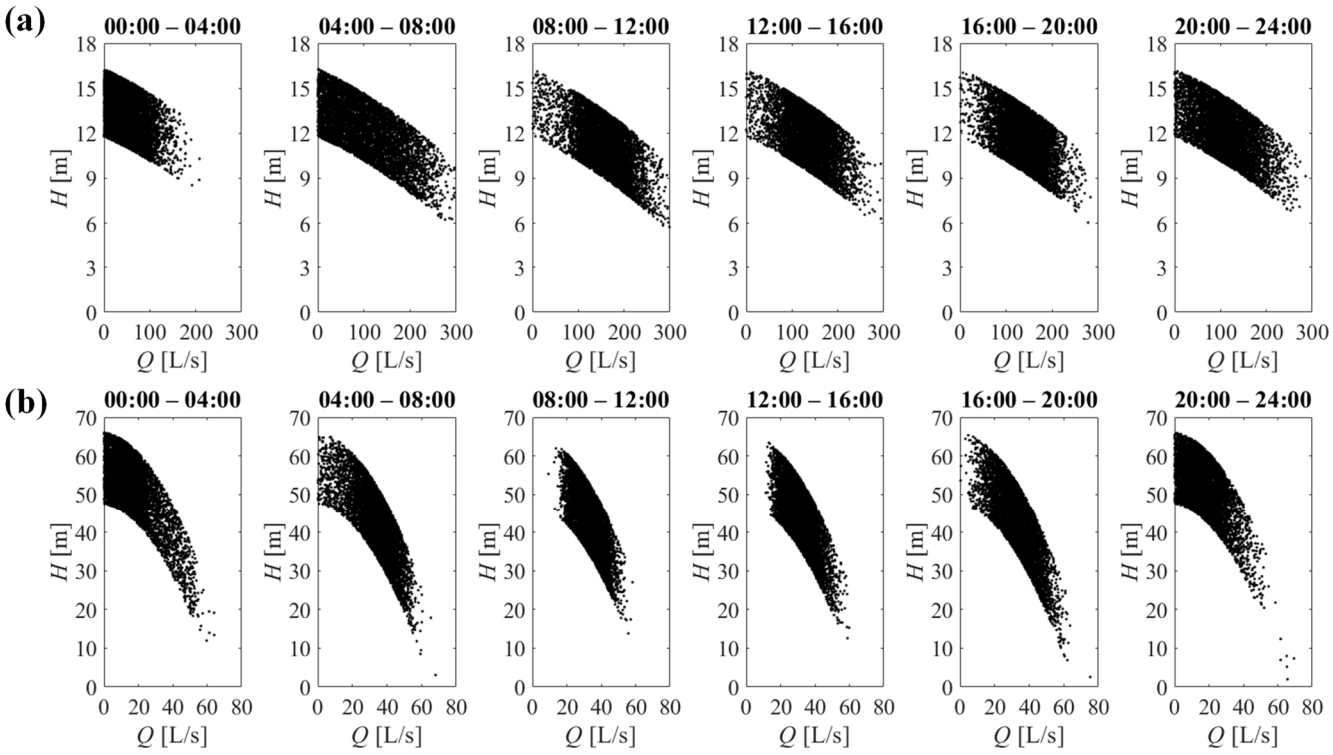

Figure 3. Q–H values for Site #1 (**a**) and Site #2 (**b**).

3.2. Pumps as Turbines

In this paper, forty-five centrifugal PATs of which the performance curves were reported in [23,34,38,44,45] are hypothetically installed at Sites #1 and #2.

Such turbomachines are employed since (i) their experimental characteristic curves are available (i.e., energy recovery is realistically evaluated); and (ii) each turbomachine operates at the same rotational speed in both direct and reverse modes (see Equations (1) and (2)). The forty-five PATs represent a heterogeneous fleet of turbomachines in terms of both geometric characteristics and operating conditions (see Figure 4 and Appendix A). In fact, the nominal impeller diameter D is in the range from 125 mm to 400 mm, while the rotational speed ranges from 600 rpm to 2700 rpm. As shown in the Appendix A, some of the considered datasets refer to the same PAT, operated at different rotational speeds.

As a result, a broad operating range is guaranteed (Figure 4). The minimum flow rate is approximately 3 L/s, while the maximum value is 110 L/s. Instead, the head drop varies from 1 m to 152 m. In general, the maximum power is lower than 20 kW with the exception of three PATs that exceed 30 kW. Finally, the efficiency ranges from 0.6% to 87.2%.

3.3. Layout of Installation

In this paper, two layouts of installation are investigated.

The first layout comprises one PAT and one bypass line, as previously shown in Figure 2a, in order to validate the methodology that selects the best PAT. Thanks to this layout, both installation and control costs are minimized [31].

The second layout includes two PATs installed in parallel (Figure 5). It must be noted that only one PAT at a time is allowed to operate. To identify the PAT that actually operates, Equations (4)–(6) are applied to both PATs. For any given time step, the PAT that operates is the one that maximizes the recovered energy, while the unexploited flow rate (if any) is swallowed through the bypass line.

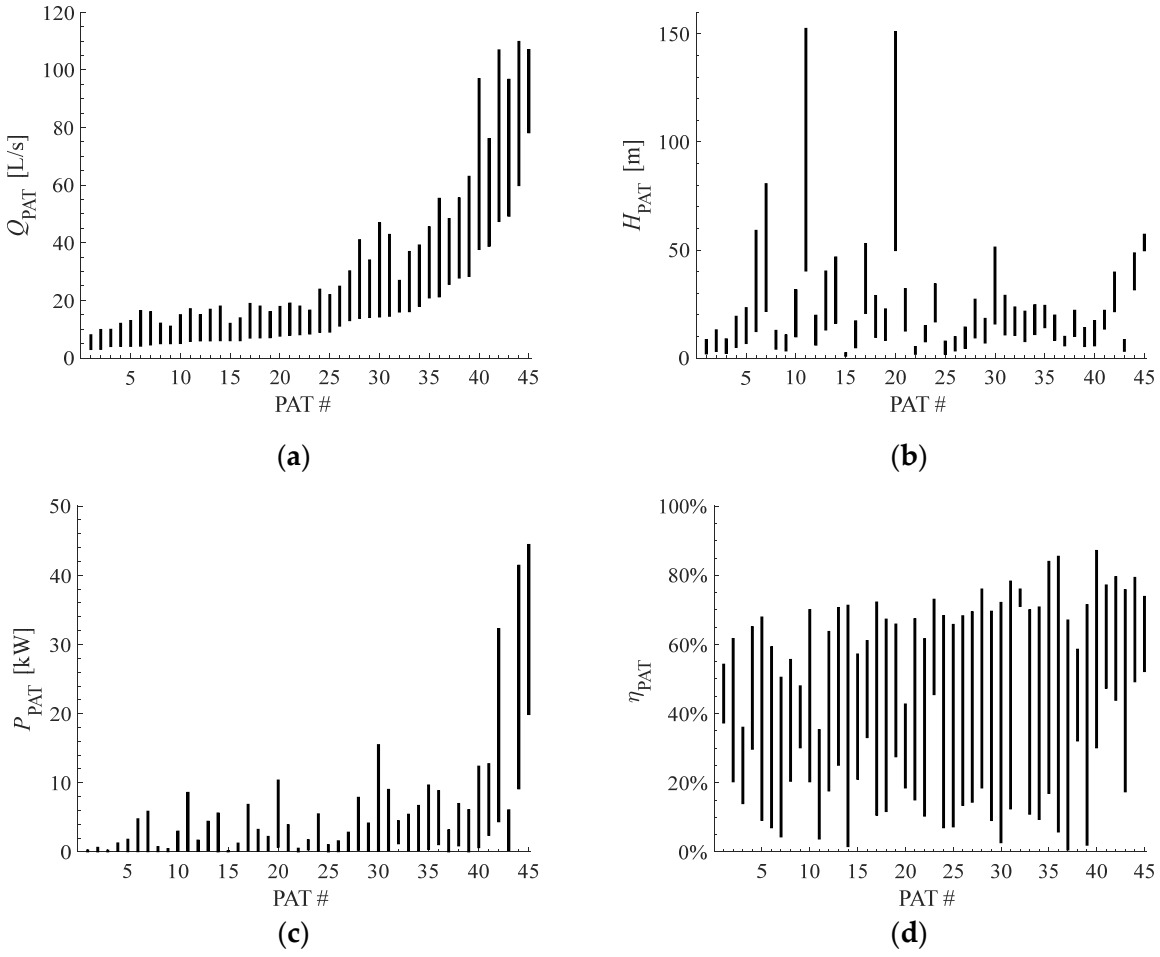

Figure 4. PAT operating ranges (volume flow rate (**a**); head (**b**); power (**c**); efficiency (**d**)).

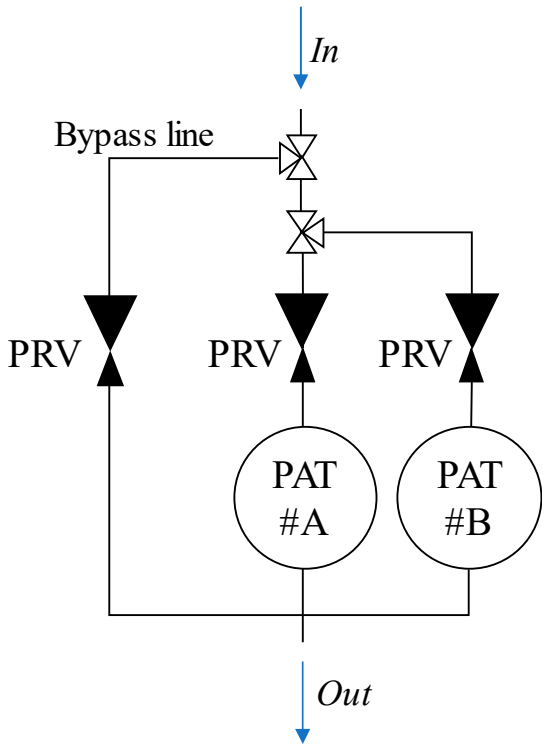

Figure 5. Layout of installation with two PATs in parallel.

4. Results

This Section addresses two goals.

Section 4.1 analyzes the installation of one PAT only (Figure 2a). First, the methodology described in Section 2 is challenged at identifying the best PAT, and the recovered energy is calculated for both sites. Finally, an in-depth analysis of optimal PAT operation is provided.

Section 4.2 instead investigates the installation of two PATs in parallel (Figure 5) to evaluate the increase in recovered energy with respect to the previous layout. To this aim, for each site, the energy recovered by means of all pairs of PATs (i.e., nine hundred ninety combinations) is calculated in order to identify the best pair of PATs.

The operation of the best PAT and best pair of PATs is discussed by analyzing (i) the range of operation of each turbomachine, (ii) the main causes of wasted energy, (iii) the time frame during which each PAT operates and (iv) the PAT's efficiency.

The rate of wasted energy due to throttle or bypass control depends on the unexploited energy calculated as in Equations (4) and (5). Thus, the rate of wasted energy is calculated as in Equations (7) and (8).

$$E_{\text{wasted,TC}} = \frac{\sum E_{\text{un,TC}}}{E_{\text{site}}} \tag{7}$$

$$E_{\text{wasted,BC}} = \frac{\sum E_{\text{un,BC}}}{E_{\text{site}}} \tag{8}$$

4.1. Single PAT

4.1.1. PAT Selection

As can be grasped from Figures 6a and 7a, the methodology described in Section 2 correctly identifies the best PAT for both sites. In fact, for Site #1 (Figure 6), twelve out of forty-five PATs were correctly filtered out, since the minimum calculated head (i.e., $H_{\text{r,T}}$) was higher than the maximum head of the site, meaning that the recovered energy would have been null (Figure 6b).

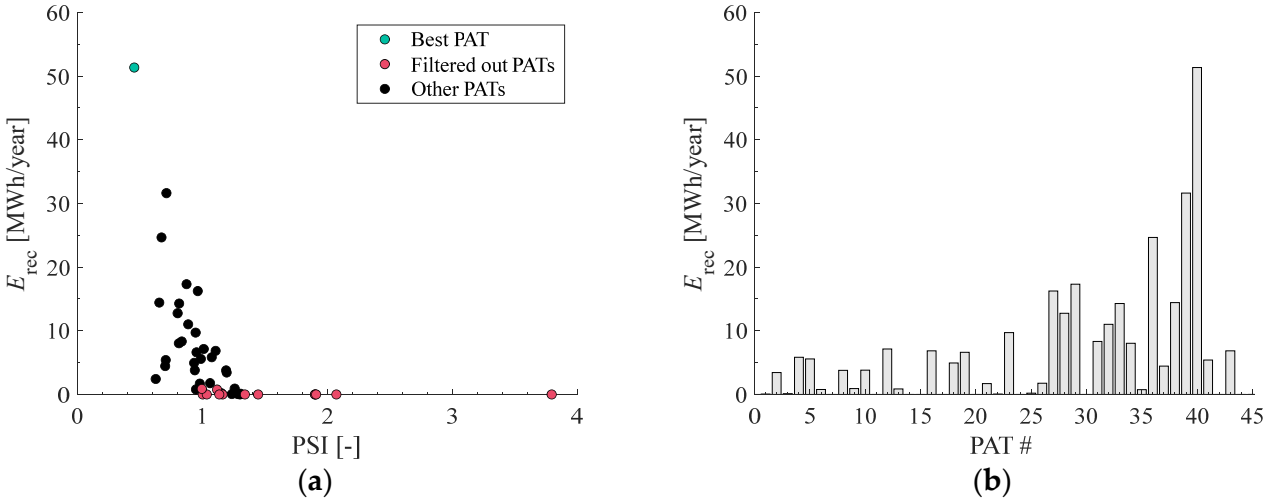

Figure 6. Recovered energy vs. PSI (**a**); energy recovered by each PAT (**b**) (Site #1).

As outlined in Figure 6a, the recovered energy tends to decrease with increasing PSI. The lowest PSI (i.e., 0.46) correctly identifies the best PAT, i.e., PAT #40, which is by far the best solution for Site #1. In fact, PAT #40 recovers 51 MWh over one year of operation, i.e., approximately 45% of the hydraulic energy of the site (Table 2). Instead, the second-best (PAT #39) and the third-best (PAT #36) solutions allow for the recovery of 28% and 22% of the hydraulic energy of the site, respectively.

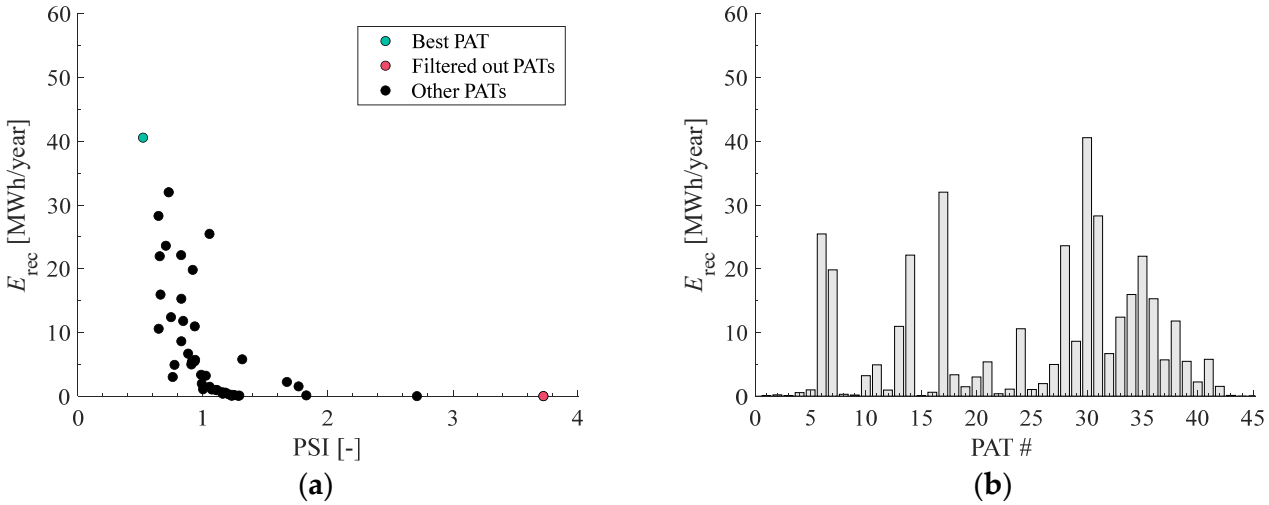

Figure 7. Recovered energy vs. PSI (**a**); energy recovered by each PAT (**b**) (Site #2).

Table 2. Recovered energy by means of the best PAT.

	Best PAT	E_{rec} **[kWh]**	E_{rec}/E_{site} **[%]**
Site #1	#40	51,341	44.8%
Site #2	#30	40,575	40.3%

For Site #2 (Figure 7), the methodology described in Section 2 preliminarily filtered out only PAT #45 of which the recovered energy is actually null.

As in Figure 6a, the recovered energy exhibits a decreasing trend with increasing *PSI* (Figure 7a). The minimum *PSI* is equal to 0.52. This allows for the correct identification of the best PAT, i.e., PAT #30, which produces 41 MWh over one year of operation. As a result, roughly 40% of the energy is recovered (Table 1). Thus, the results obtained for both Site #1 and Site #2 validate the methodology proposed by Manservigi et al. [31], since the minimum PSI correctly identifies the best PAT at both sites.

4.1.2. PAT Operation

The operation of the best PAT is discussed in the following to grasp recommendations to further increase energy recovery.

At Site #1, PAT #40 operates between 37.7 L/s and 89.5 L/s (red symbols in Figure 8a), while the head varies from 5.6 m to 14.8 m. PAT #40 recovers only 44.8% of the available energy (Figure 8b). This is mainly due to the bypass control, which wastes 47.9% of the energy, while the throttle control wastes only 4.9% of the site energy.

Finally, only a small amount of energy (i.e., 2.4%) is not recovered because the PAT does not operate (i.e., the flow rate is below the runaway condition). In more detail, PAT #40 does not operate, mainly during nighttime, because of low flow rates. Starting from 04:00, the PAT's operation significantly increases and is constant up to 20:00. Then, it decreases again (Figure 8c). The analysis, as shown in Figure 8d, reveals that the PAT's efficiency is usually higher than 80%.

In conclusion, these findings clearly outline that PAT #40 is a suitable turbomachine for Site #1. However, the recovered energy is relatively low because of the energy wasted due to the bypass control, which, according to Figure 8b, is the largest source of loss.

At Site #2, PAT #30 does not operate when the site flow rate and head are lower than the runaway condition (Figure 9a), which wastes 6.3% of the energy (Figure 9b).

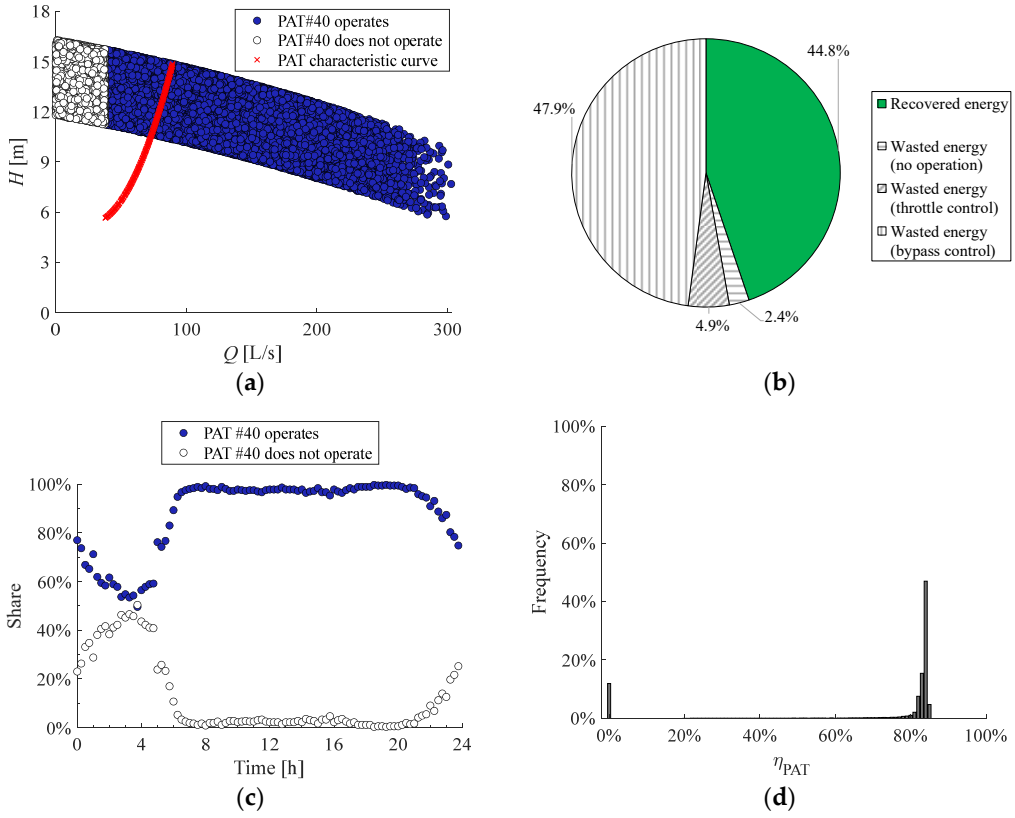

Figure 8. Operation of PAT #40 (**a**); share of recovered and wasted energy at Site #1 (**b**); share of PAT's operation (PAT #40) (**c**); efficiency of PAT #40 (**d**).

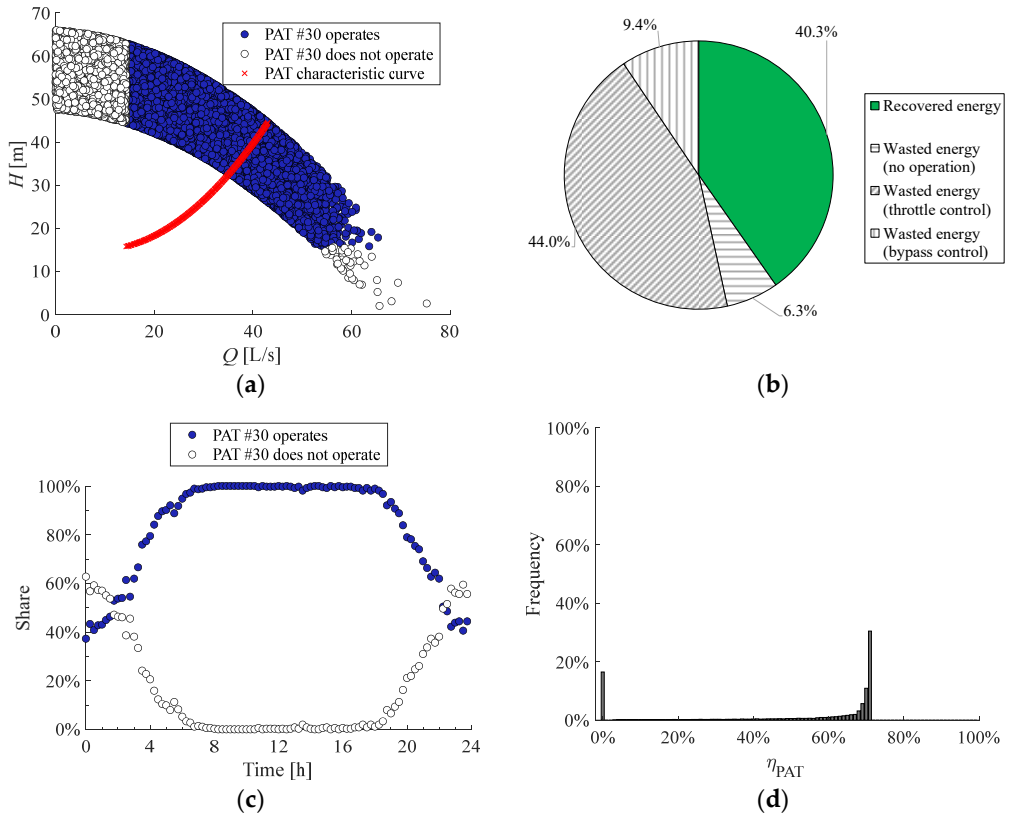

Figure 9. Operation of PAT #37 (**a**); share of recovered and wasted energy at Site #2 (**b**); share of PAT's operation (PAT#30) (**c**); efficiency of PAT #30 (**d**).

As mentioned for Site #1, such a scenario mainly occurs during nighttime (Figure 9c). Most of the energy is wasted because of both throttle and bypass controls, which waste 44.0% and 9.4% of the energy, respectively. As a result, 40.3% of the energy is recovered.

Finally, Figure 9d outlines that the PAT efficiency is null (i.e., PAT #30 does not operate) in 16.5% of cases, while η_{PAT} varies from 3.5% to 71.8% (i.e., the BEP). Although, in this paper, PAT #30 is allowed to explore its entire range of operation, η_{PAT} is in the range from 71% to 71.8% in 30.5% of cases.

In conclusion, PAT #30 is a suitable turbomachine for Site #2. However, a second PAT installed in parallel is expected to significantly increase the rate of recovered energy, mainly by reducing the amount of energy wasted because of throttle control.

4.2. Pair of PATs in Parallel

The analysis of all PAT combinations highlights two main findings.

First, as shown in Figure 10, the exploitation of two PATs, if not properly selected, is not always advantageous with respect to the use of just one "optimal" PAT.

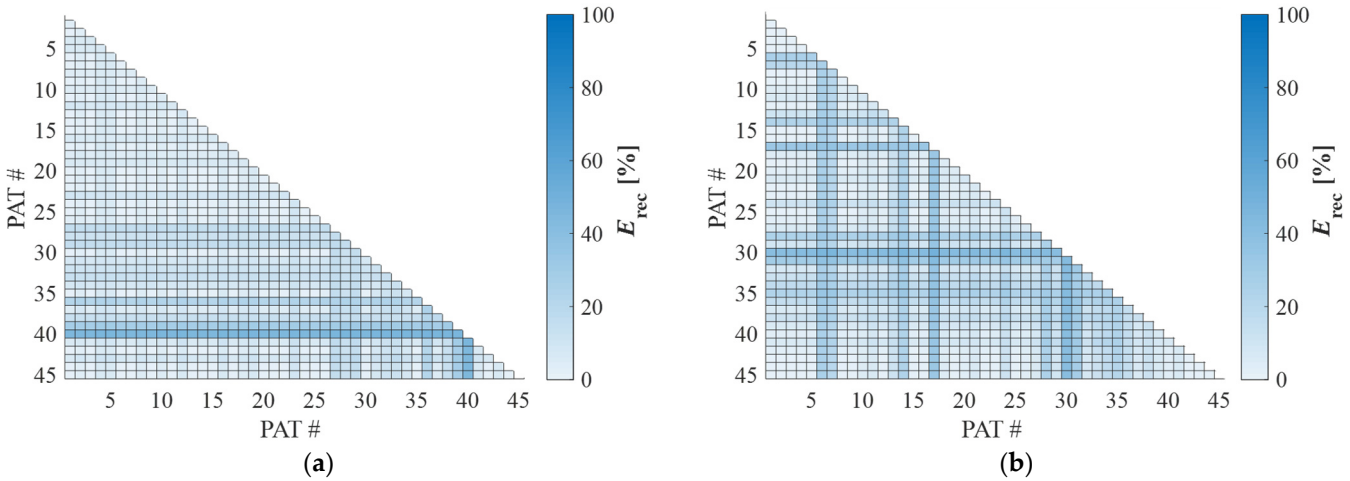

Figure 10. Rate of recovered energy by means of all pairs of PATs (Site#1 (**a**); Site#2 (**b**)).

In other words, there are several pairs of PATs that allow for the recovery of less energy than a single PAT. This outcome is demonstrated at both sites.

Such a result proves that a pair of PATs must be properly selected to guarantee an actual gain of energy recovery with respect to a single PAT.

Second, for both sites, the best pair of PATs comprises the "best single" PAT. In fact, for Site #1, the best pair is composed of PATs #40 and #36, while PATs #30 and #17 are the best options for Site #2 (Table 3).

Table 3. Recovered energy by means of the best pair of PATs.

	Best Pair of PAT	E_{rec} [kWh]	E_{rec}/E_{site} [%]
Site #1	#40, #36	53,695	46.9%
Site #2	#30, #17	49,605	49.3%

At Site #1, the best pair of PATs (i.e., PATs #40–#36) only slightly increases the rate of recovered energy with respect to PAT #40 by passing from 44.8% (Table 2) to 46.9% (Table 3). However, it should be observed that the energy recovered by the other four pairs of PATs (i.e., PATs #40–#28, PATs #40–#29, PATs #40–#32, PATs #40–#33 (Figure 10a)) is higher than 46.0%. This outcome can be explained by the fact that PAT #40 optimally fits the characteristics of Site #1, while the second PAT mainly operates at low flow rates (Figure 11a). When the site flow rate is lower than 28.1 L/s, both PATs do not operate, which wastes only 1.2% of the energy (Figure 11b). PAT #36 also reduces the amount of

energy lost due to throttle control, which passes from 4.9% (Figure 8b) to 2.5% (Figure 11b). Conversely, the energy wasted because of bypass control increases up to 49.4% (Figure 11b).

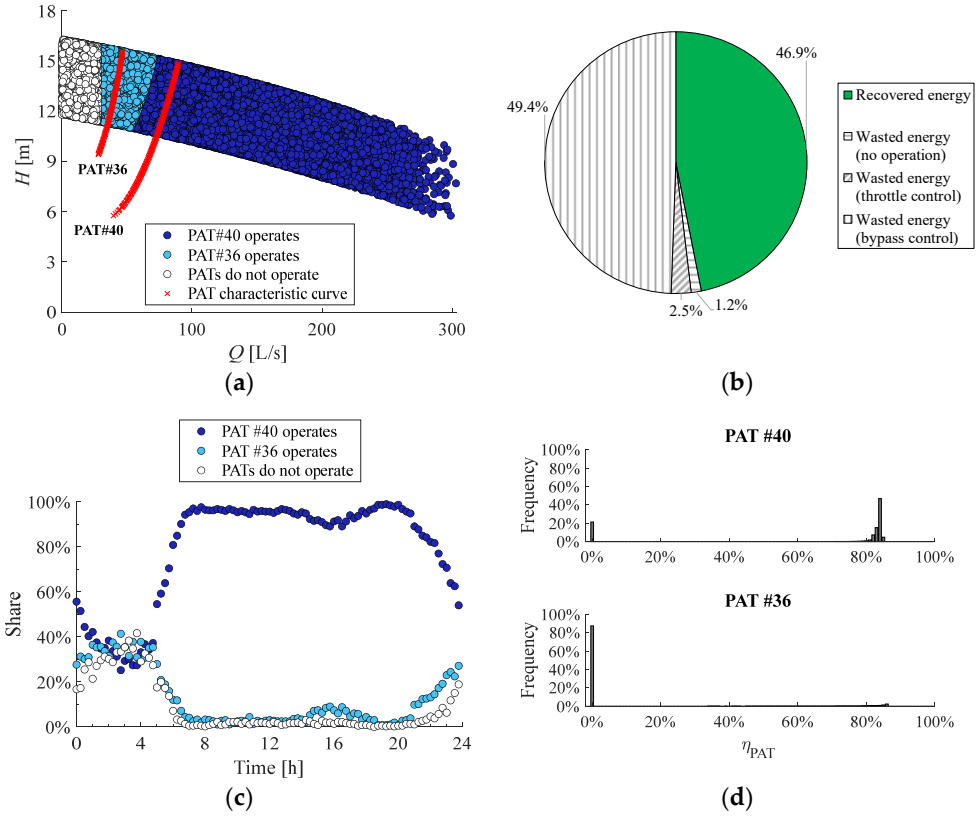

Figure 11. Operation of PATs #40 and #36 (**a**); share of recovered and wasted energy at Site #1 (**b**); share of PAT's operation (PATs #40 and #36) (**c**); efficiency of PATs #40 and #36 (**d**).

By analyzing the time of operation (Figure 11c), it is clear that PAT #40 mainly runs during daytime. Instead, the share of operation of both PATs is almost the same from 00:00 to 04:00.

Finally, PAT #40 frequently runs close to its BEP, while PAT #36 reaches its BEP only 2.4% of the time (Figure 11d). However, it has to be mentioned that PAT #36 is only occasionally exploited.

Thus, based on these comments, the benefits of installing two PATs are limited.

At Site #2, the exploitation of two PATs is extremely favorable from an energy point of view. In fact, the recovered energy increases from 40.3% (i.e., PAT #30 only) to 49.3% (i.e., best pair of PATs). The best pair of PATs (i.e., PATs #30–#17) is by far the best solution, since the second-best alternative is represented by PATs #30–#6, which recover 46.7% of the energy. The relevant increase in recovered energy is mainly due to the optimal management of both PATs. First, PAT #17 mainly operates at low flow rates since its runaway condition occurs at a lower flow rate than that of PAT #30 (Figure 12a). As a result, only 1.2% of the site energy is lost (Figure 12b). Instead, PAT #30 maximizes the energy recovered at high flow rates. The throttle control dissipates most of the hydraulic energy (29.4%), followed by the bypass control (20.1%) (Figure 12b). This result is in agreement with the range of operation of PAT #17 (Figure 12a).

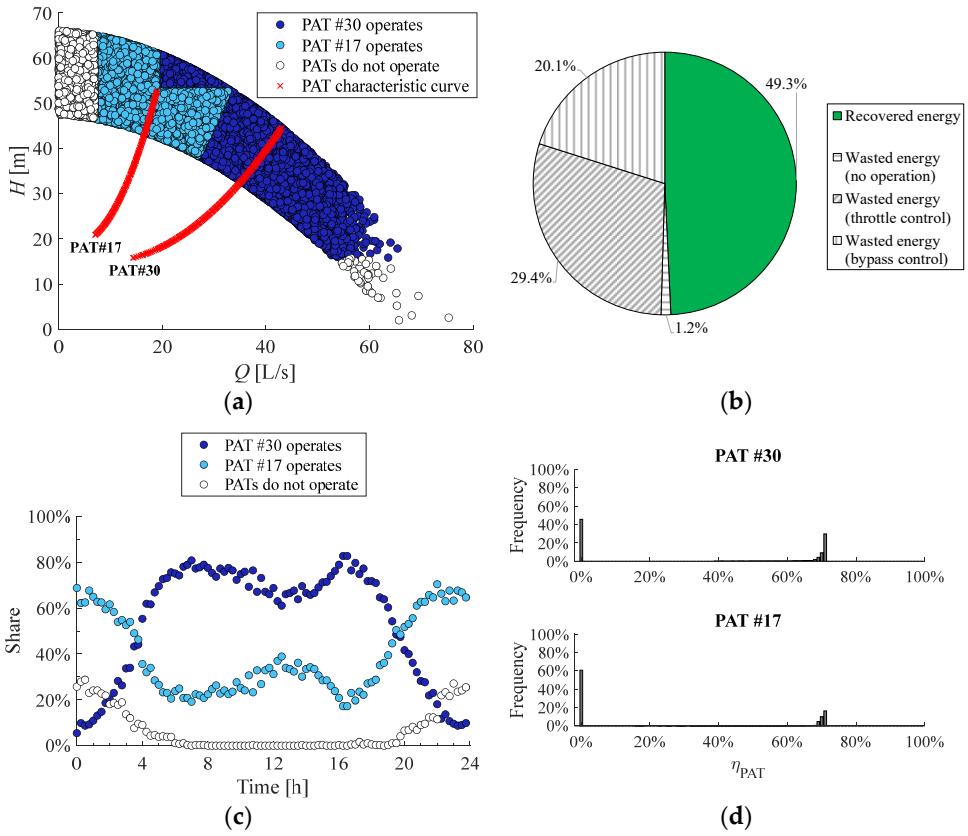

Figure 12. Operation of PATs #30 and #17 (**a**); share of recovered and wasted energy at Site #2 (**b**); share of PAT's operation (PATs #30 and #17) (**c**); efficiency of PATs #30 and #17 (**d**).

An in-depth analysis of PAT operation reveals that PAT #17 mainly operates during nighttime (Figure 12c). For example, PAT #17 operates at midnight 68.8% of the time. The frequency of PAT #17 operation decreases over time, and then, it increases again. Conversely, PAT #30 mainly runs during daytime, especially at 16:30, at which it operates in 82.7% of cases (Figure 12c).

As can be grasped from Figure 12d, PAT #30 works more frequently than PAT #17 since it operates 44.3% of the year (see Figure 12d), while PAT #17 runs 39.2% of the year. In addition, although it cannot be clearly observed in Figures 9d and 12d, PAT #30 works more efficiently, since PAT #17 tends to operate when the efficiency of PAT #30 is lower than 40%. Finally, both PATs usually operate close to their BEPs, which are approximately equal to 72% (Figure 12d).

Based on these comments, the installation of two PATs working in parallel is highly recommend from the point of view of energy recovery, since for this hydraulic site, they are complementary.

5. Conclusions

A pump as turbine (PAT) is a cost-effective and versatile solution to recover hydraulic energy in several fields of application. However, its installation is generally limited by the fact that a reliable methodology aimed at selecting the best PAT, i.e., the one that maximizes the recovered energy, is still not consolidated in the literature.

This paper presented a methodology, previously developed by the same authors, aimed at selecting the best PAT that, in parallel with a bypass line, can accomplish either throttle or bypass control.

The methodology comprises two steps. First, the runaway condition has to be identified to filter out the PATs that are not suitable for a given hydraulic site. Then, the lowest PAT–site index (PSI) is used to identify the best PAT.

First, this paper validated such a methodology by means of two hydraulic sites and a fleet of forty-five heterogeneous PATs of which the experimental performance curves were available in the literature. At both sites, energy recovery increased by lowering the PSI, and the best PAT was correctly identified. Thus, the methodology proved to be fully reliable.

Over one year of operation, the best PAT allowed for the recovery of approximately 51 MWh (Site #1) and 41 MWh (Site #2), i.e., 44.8% and 40.3% of the hydraulic energy, respectively. At Site #1, the best PAT wasted the most energy (i.e., 47.9%) due to the throttle control, and it mainly ran during daytime nearby its best efficiency point. Also, at Site #2, the best PAT mainly operated during daytime nearby its best efficiency point, but 44% of the energy was lost because of the throttle control.

Then, a second layout of installation, which comprised two PATs installed in parallel and one bypass line, was also investigated. At each time step, the PAT in operation was imposed to be the one that maximized the recovered energy. It was found that all best pairs of PATs included the best single PAT, thus reinforcing the capability of the methodology when a pair of PATs is employed.

At Site #1, the best pair of PATs only slightly increased energy recovery, which passed from 51 MWh to 54 MWh. Thus, 46.9% of the available energy was recovered. In this scenario, one PAT occasionally ran, and thus, the benefits of installing two PATs were limited. At Site #2, the best pair of PATs increased energy recovery up to 50 MWh (i.e., 49.3% of the available energy), as each PAT mainly operated during a specific time slot (i.e., daytime or nighttime). When operating, both PATs frequently ran nearby the respective best efficiency point. Thus, the installation of two PATs was actually recommended.

Future analyses are planned to investigate both layouts of installation from an economic point of view. In addition, energy recovery by means of speed control will also be investigated.

Author Contributions: Conceptualization, L.M. and M.V.; methodology, L.M.; software, L.M.; validation, L.M., M.V., E.L. and G.A.M.C.; formal analysis, L.M.; investigation, L.M.; writing—original draft preparation, L.M.; writing—review and editing, L.M., M.V., E.L. and G.A.M.C.; visualization, L.M., M.V., E.L. and G.A.M.C. All authors have read and agreed to the published version of the manuscript.

Funding: This paper was carried out in the framework of the project funded under (i) the National Recovery and Resilience Plan (NRRP), Mission 04 Component 2 Investment 1.5—NextGenerationEU, Call for tender n. 3277 dated 30 December 2021. Award Number: 0001052 dated 23 June 2022; (ii) FIRD 2022—Gestione sostenibile, recupero energetico e controllo ottimizzato di reti idriche urbane mediante PAT; (iii) Bando Giovani anno 2022 per progetti di ricerca finanziati con il contributo 5x1000 anno 2021.

Data Availability Statement: Data will be made available on request.

Conflicts of Interest: The authors declare no conflict of interest.

Nomenclature

D	diameter
E	energy
g	gravitational acceleration
H	head
N	rotational speed
P	power
PSI	PAT–site index
Q	flow rate
t	time
η	efficiency
ρ	density
Subscripts	
BEP	best efficiency point
max	maximum value

mean	mean value
P	pump mode
r	runaway condition
rec	recovered
ref	reference value
T	turbine mode
un	unexploited
Acronyms	
BC	Bypass Control
BEP	Best Efficiency Point
PAT	Pump As Turbine
PRV	Pressure Reducing Valve
PSI	PAT–Site Index
TC	Throttle Control

Appendix A

Table A1. Pump/PAT characteristics and BEPs.

			PUMP		PAT		
PAT #	***D* [m]**	***N* [rpm]**	**Q_{BEP} [L/s]**	**H_{BEP} [m]**	**Q_{BEP} [L/s]**	**H_{BEP} [m]**	**Ref.**
1	0.160	600	2.96	1.36	5.01	3.80	[45]
2	0.160	900	3.98	2.95	5.99	5.51	[45]
3	0.125	600	2.86	0.96	7.04	4.62	[45]
4	0.160	1200	4.33	5.65	7.08	8.45	[45]
5	0.160	1500	5.95	8.04	9.07	13.22	[45]
6	0.200	1450	5.87	11.51	9.60	25.14	[23]
7	0.250	1450	6.76	19.57	9.63	37.17	[23]
8	0.125	1200	5.03	2.90	9.13	7.60	[45]
9	0.125	900	3.98	1.70	7.99	5.86	[45]
10	0.160	1800	6.97	11.53	11.02	19.47	[45]
11	0.315	1450	7.54	31.38	14.10	110.64	[23]
12	0.125	1800	5.97	7.18	11.05	11.66	[45]
13	0.160	2100	8.00	15.66	13.09	27.06	[45]
14	0.160	2400	9.97	19.48	15.00	35.38	[45]
15	0.125	600	5.49	0.76	9.02	1.39	[45]
16	0.125	1500	5.98	4.55	10.05	9.33	[45]
17	0.160	2700	10.96	24.92	16.02	41.14	[45]
18	0.125	2400	7.99	12.20	15.00	20.80	[45]
19	0.125	2100	7.02	9.40	13.10	15.92	[45]
20	0.335	1450	7.99	31.29	13.71	99.54	[23]
21	0.125	2700	9.00	15.34	16.03	23.99	[45]
22	0.125	900	7.96	1.64	13.98	3.20	[45]
23	0.160	1450	9.72	8.55	15.27	13.10	[23]
24	0.250	1450	18.58	17.97	23.01	32.66	[23]
25	0.125	1200	11.00	2.84	18.10	5.38	[45]
26	0.125	1500	13.86	4.28	21.95	7.72	[45]
27	0.125	1800	16.61	6.13	25.95	10.97	[45]
28	0.200	1450	23.28	12.07	31.25	17.56	[23]
29	0.125	2100	19.00	8.38	29.90	14.48	[45]
30	0.250	1450	26.77	19.70	33.15	30.15	[23]
31	0.220	1450	24.15	14.54	32.70	19.25	[23]
32	0.193	1450	14.00	10.00	21.00	14.70	[38]
33	0.125	2400	21.79	10.79	33.99	18.61	[45]
34	0.125	2700	24.47	13.68	39.23	24.69	[45]
35	0.269	1450	40.25	22.26	45.82	24.40	[44]
36	0.219	1450	41.68	13.78	50.33	17.29	[44]
37	0.160	1450	41.98	7.91	48.44	10.04	[23]
38	0.200	1450	41.68	12.96	50.00	18.83	[23]

Table A1. *Cont.*

			PUMP		PAT		
PAT #	***D* [m]**	***N* [rpm]**	Q_{BEP} **[L/s]**	H_{BEP} **[m]**	Q_{BEP} **[L/s]**	H_{BEP} **[m]**	**Ref.**
39	0.185	1450	41.62	7.72	59.83	12.93	[44]
40	0.200	1450	70.04	13.99	76.09	11.22	[23]
41	0.400	800	60.21	17.59	76.18	22.11	[34]
42	0.400	1000	75.14	26.90	96.60	34.71	[34]
43	0.224	1050	72.36	5.41	94.39	8.42	[44]
44	0.400	1200	102.12	36.21	98.70	44.13	[34]
45	0.400	1520	129.79	56.90	107.07	57.30	[34]

References

1. Ali, A.; Yuan, J.; Javed, H.; Si, Q.; Fall, I.; Ohiemi, I.E.; Osman, F.K.; Islam, R. Small hydropower generation using pump as turbine; a smart solution for the development of Pakistan's energy. *Heliyon* **2023**, *9*, 14993. [CrossRef] [PubMed]
2. Nejadali, J. Analysis and evaluation of the performance and utilization of regenerative flow pump as turbine (PAT) in Pico-hydropower plants. *Energy Sustain. Dev.* **2021**, *64*, 103–117. [CrossRef]
3. Carravetta, A.; Derakhshan Houreh, S.; Ramos, H.M. *Pumps as Turbines*, 1st ed.; Springer International Publishing: Cham, Switzerland, 2018.
4. Spedaletti, S.; Rossi, M.; Comodi, G.; Salvi, D.; Renzi, M. Energy recovery in gravity adduction pipelines of a water supply system (WSS) for urban areas using Pumps-as-Turbines (PaTs). *Sustain. Energy Technol. Assess.* **2021**, *45*, 101040. [CrossRef]
5. Ramos, H.M.; Morani, M.C.; Pugliese, F.; Fecarotta, O. Integrated Smart Management in WDN: Methodology and Application. *Water* **2023**, *15*, 1217. [CrossRef]
6. Le Marre, M.; Mandin, P.; Lanoisellé, J.; Zilliox, E.; Rammal, F.; Kim, M.; Inguanta, R. Pumps as turbines regulation study through a decision-support algorithm. *Renew. Energy* **2022**, *194*, 561–570. [CrossRef]
7. Ávila, C.A.M.; Sánchez-Romero, F.; López-Jiménez, P.A.; Pérez-Sánchez, M. Optimization tool to improve the management of the leakages and recovered energy in irrigation water systems. *Agric. Water Manag.* **2021**, *258*, 107223. [CrossRef]
8. Venturini, M.; Alvisi, S.; Simani, S.; Manservigi, L. Energy Production by Means of Pumps as Turbines in Water Distribution Networks. *Energies* **2017**, *10*, 1666. [CrossRef]
9. Hanaei, S.; Lakzian, E. Numerical and experimental investigation of the effect of the optimal usage of pump as turbine instead of pressure-reducing valves on leakage reduction by genetic algorithm. *Energy Convers. Manag.* **2022**, *270*, 116253. [CrossRef]
10. Postacchini, M.; Darvini, G.; Finizio, F.; Pelagalli, L.; Soldini, L.; Di Giuseppe, E. Hydropower generation through pump as turbine: Experimental study and potential application to small-scale WDN. *Water* **2020**, *12*, 958. [CrossRef]
11. Postacchini, M.; Di Giuseppe, E.; Eusebi, A.L.; Pelagalli, L.; Darvini, G.; Cipolletta, G.; Fatone, F. Energy saving from small-sized urban contexts: Integrated application into the domestic water cycle. *Renew. Energy* **2022**, *199*, 1300–1317. [CrossRef]
12. Sarbu, I.; Mirza, M.; Muntean, D. Integration of Renewable Energy Sources into Low-Temperature District Heating Systems: A Review. *Energies* **2022**, *15*, 6523. [CrossRef]
13. García, A.M.; Gallagher, J.; Chacón, M.C.; Mc Nabola, A. The environmental and economic benefits of a hybrid hydropower energy recovery and solar energy system (PAT-PV), under varying energy demands in the agricultural sector. *J. Clean. Prod.* **2021**, *303*, 127078. [CrossRef]
14. Ji, Y.; Ran, J.; Yang, Z.; Li, H.; Hao, X. Optimization of energy recovery turbine in demineralized water treatment system of power station by Box–Behnken Design method. *Energy Rep.* **2022**, *8*, 362–370. [CrossRef]
15. Wang, H.; Wang, F.; Wang, B.; Wang, C.; Wu, J.; Lu, H. Gravity-induced virtual clocking effect in large-capacity/low-head pumped hydro energy storage system with horizontal shaft. *Sustain. Energy Technol. Assess.* **2023**, *60*, 103441. [CrossRef]
16. Balacco, G.; Fiorese, G.D.; Alfio, M.R.; Totaro, V.; Binetti, M.; Torresi, M.; Stefanizzi, M. PaT-ID: A tool for the selection of the optimal pump as turbine for a water distribution network. *Energy* **2023**, *282*, 128366. [CrossRef]
17. Marini, G.; Di Menna, F.; Maio, M.; Fontana, N. HYPER: Computer-Assisted Optimal Pump-as-Turbine (PAT) Selection for Microhydropower Generation and Pressure Regulation in a Water Distribution Network (WDN). *Water* **2023**, *15*, 2807. [CrossRef]
18. European Commission. *Proposal for a Directive of the European Parliament and of the Council on the Quality of Water Intended for Human Consumption (Recast)*; European Commission: Brussels, Belgium, 2018.
19. Stefanizzi, M.; Filannino, D.; Capurso, T.; Camporeale, S.M.; Torresi, M. Optimal hydraulic energy harvesting strategy for PaT installation in Water Distribution Networks. *Appl. Energy* **2023**, *344*, 121246. [CrossRef]
20. Novara, D.; McNabola, A. Design and Year-Long Performance Evaluation of a Pump as Turbine (PAT) Pico-Hydropower Energy Recovery Device in a Water Network. *Water* **2021**, *13*, 3014. [CrossRef]
21. Pugliese, F.; Giugni, M. An Operative Framework for the Optimal Selection of Centrifugal Pumps as Turbines (PATs) in Water Distribution Networks (WDNs). *Water* **2022**, *14*, 1785. [CrossRef]
22. Nasir, A.; Dribssa, E.; Girma, M.; Madessa, H.B. Selection and Performance Prediction of a Pump as a Turbine for Power Generation Applications. *Energies* **2023**, *16*, 5036. [CrossRef]

23. Barbarelli, S.; Amelio, M.; Florio, G. Experimental activity at test rig validating correlations to select pumps running as turbines in microhydro plants. *Energy Convers. Manag.* **2017**, *149*, 781–797. [CrossRef]
24. Kostner, M.K.; Zanfei, A.; Alberizzi, J.C.; Renzi, M.; Righetti, M.; Menapace, A. Micro hydro power generation in water distribution networks through the optimal pumps-as-turbines sizing and control. *Appl. Energy* **2023**, *351*, 121802. [CrossRef]
25. Fernández García, I.; Ferras, D.; McNabola, A. Potential of energy recovery and water saving using micro-hydropower in rural water distribution networks. *J. Water Resour. Plan. Manag.* **2019**, *145*, 1–11. [CrossRef]
26. Fernández García, I.; Mc Nabola, A. Maximizing hydropower generation in gravity water distribution networks: Determining the optimal location and number of pumps as turbines. *J. Water Resour. Plan. Manag.* **2020**, *146*, 04019066. [CrossRef]
27. Pérez-Sánchez, M.; Sánchez-Romero, F.J.; López Jiménez, P.A.; Ramos, H.M. PATs selection towards sustainability in irrigation networks: Simulated annealing as a water management tool. *Renew. Energy* **2018**, *116*, 234–249. [CrossRef]
28. Mercedes-García, A.V.; Sánchez-Romero, F.J.; López Jiménez, P.A.; Pérez-Sánchez, M. A new optimization approach for the use of hybrid renewable systems in the search of the zero net energy consumption in water irrigation systems. *Renew. Energy* **2022**, *195*, 853–871. [CrossRef]
29. Chacón, M.C.; Rodríguez Díaz, J.A.; García Morillo, J.; McNabola, A. Pump-as-turbine selection methodology for energy recovery in irrigation networks: Minimising the payback period. *Water* **2019**, *11*, 149. [CrossRef]
30. Pérez-Sánchez, M.; Sánchez-Romero, F.J.; Ramos, H.M.; López Jiménez, P.A. Optimization Strategy for Improving the Energy Efficiency of Irrigation Systems by Micro Hydropower: Practical Application. *Water* **2017**, *9*, 799. [CrossRef]
31. Manservigi, L.; Venturini, M.; Losi, E. Optimal selection of pumps as turbines for maximizing electrical energy production. In Proceedings of the 100RES 2020—Applied Energy Symposium (ICAE) 100% RENEWABLE: Strategies, Technologies and Challenges for a Fossil Free Future, Pisa, Italy, 25–30 October 2020.
32. Gulich, J.F. *Centrifugal Pumps*, 3rd ed.; Springer: Berlin/Heidelberg, Germany, 2014.
33. Kandi, A.; Moghimi, M.; Tahani, M.; Derakhshan, S. Efficiency Increase in Water Transmission Systems Using Optimized Selection of Parallel Pumps Running as Turbines. *J. Water Resour. Plan. Manag.* **2021**, *147*, 04021065. [CrossRef]
34. Stefanizzi, M.; Capurso, T.; Balacco, G.; Torresi, M.; Binetti, M.; Piccinni, A.F.; Fortunato, B.; Camporeale, S.M. Preliminary assessment of a pump used as turbine in a water distribution network for the recovery of throttling energy. In Proceedings of the 12th European Conference on Turbomachinery Fluid dynamics & Thermodynamics ETC13, Lausanne, Switzerland, 8–12 April 2018.
35. Creaco, E.; Campisano, A.; Fontana, N.; Marini, G.; Page, P.R.; Walski, T. Real time control of water distribution networks: A state-of-the-art review. *Water Res.* **2019**, *161*, 517–530. [CrossRef] [PubMed]
36. Castorino, G.A.M.; Manservigi, L.; Barbarelli, S.; Losi, E.; Venturini, M. Development and validation of a comprehensive methodology for predicting PAT performance curves. *Energy* **2023**, *274*, 127366. [CrossRef]
37. Venturini, M.; Manservigi, L.; Alvisi, S.; Simani, S. Development of a physics-based model to predict the performance of pumps as turbines. *Appl. Energy* **2018**, *213*, 343–354. [CrossRef]
38. Rossi, M.; Nigro, A.; Renzi, M. Experimental and numerical assessment of a methodology for performance prediction of Pumps-as-Turbines (PaTs) operating in off-design conditions. *Appl. Energy* **2019**, *248*, 555. [CrossRef]
39. Cao, Z.; Deng, J.; Zhao, L.; Lu, L. Numerical Research of Pump-as-Turbine Performance with Synergy Analysis. *Processes* **2021**, *9*, 1031. [CrossRef]
40. Venturini, M.; Alvisi, S.; Simani, S.; Manservigi, L. Comparison of Different Approaches to Predict the Performance of Pumps as Turbines (PATs). *Energies* **2018**, *11*, 1016. [CrossRef]
41. Brisbois, A.; Dziedzic, R. Multivariate Regression Models for Predicting Pump-as-Turbine Characteristics. *Water* **2023**, *15*, 3290. [CrossRef]
42. Yang, S.S.; Derakhshan, S.; Kong, F.Y. Theoretical, numerical and experimental prediction of pump as turbine performance. *Renew. Energy* **2012**, *48*, 507–513. [CrossRef]
43. Yang, F.; Li, Z.; Cai, Y.; Jiang, D.; Tang, F.; Sun, S. Numerical Study for Flow Loss Characteristic of an Axial-Flow Pump as Turbine via Entropy Production Analysis. *Processes* **2022**, *10*, 1695. [CrossRef]
44. Tan, X.; Engeda, A. Performance of centrifugal pumps running in reverse as turbine: Part II- systematic specific speed and specific diameter based performance prediction. *Renew. Energy* **2016**, *99*, 188–197. [CrossRef]
45. Delgado, J.; Ferreira, J.P.; Covas, D.I.C.; Avellan, F. Variable speed operation of centrifugal pumps running as turbines. Experimental investigation. *Renew. Energy* **2019**, *142*, 437–450. [CrossRef]